Fluoxetine Delivery for Wound Treatment Through an Integrated Bioelectronic Device – Pharmacokinetic Parameters and Safety Profile in Swine

Anthony Gallegos[1], Houpu Li[2], Hsin-ya Yang[1], Guillermo Villa-Martinez[1], Itidal Bazzi[1], Samhitha Sathyanarayanan[1], Narges Asefifeyzabadi[2], Prabhat Baniya[2], Wan Shen Hee[2], Mohammadhosein Siadat[1], Elizabeth Chang[1], Sriansh Pasumarthi[1], Mircea Teodorescu[2], Marcella Gomez[3], Marco Rolandi*[2], Rivkah Isseroff*[1]

[1]Department of Dermatology, School of Medicine, University of California Davis, Davis, CA 95616, USA

[2]Department of Electrical and Computer Engineering, University of California Santa Cruz, Santa Cruz, CA 95064, USA

[3]Department of Applied Mathematics, University of California Santa Cruz, Santa Cruz, CA 95060, USA

*Corresponding authors. Email: rrisseroff@ucdavis.edu, mrolandi@ucsc.edu

Abstract

Wound infections are a significant medical challenge, often leading to chronicity or systemic infection. Selective serotonin reuptake inhibitors (SSRIs) have emerged as potential non-antibiotic candidates with demonstrated ability to limit growth and biofilm formation in Gram-negative bacteria, in addition to their pro-healing activity. Here, we compared direct delivery of the SSRI fluoxetine by topical bolus dosing to delivery from an iontophoresis bandage device with an actuator for temporally controlled drug delivery, in a porcine excisional wound model. Device delivery of fluoxetine resulted in a maximum concentration of 12.25 ng fluoxetine per mg tissue, compared to 2.926 ng/mg following bolus dosing, and tissue fluoxetine levels were higher after application using the device than after bolus dosing across the range of doses tested ($p=0.0041$). The half-life of fluoxetine in the wound tissue was 0.988 ± 0.256 days. Fluoxetine was not detected in the pig plasma, and plasma serotonin levels were not affected by the topical application. Fluoxetine delivery using the device, but not bolus delivery, produced tissue concentrations above the minimum inhibitory concentration (MIC) for some clinically important species of bacteria.

The experimental device can effectively deliver topical fluoxetine to the wound, producing higher tissue concentrations of fluoxetine at lower cumulative doses compared to bolus dosing, and with minimal risk of off-target effects. The device may simplify wound treatment by reducing the burden for daily drug application, possibly increasing adherence to a prescribed treatment regimen.

Translational Impact Statement

We developed a bioelectronic wound management device to deliver fluoxetine, a repurposed SSRI drug, to wounds. Fluoxetine has potential applications in normal wound healing and as an adjunctive therapy for infected wounds. Device delivery of fluoxetine was compared to conventional bolus dosing in a pig excisional wounding model. Some pharmacokinetic parameters and the safety profile of topical fluoxetine wound therapy were established.

Keywords
Wound healing, fluoxetine, bioelectronics, pharmacokinetics, drug repurposing, wound infection

Introduction

Skin wounds, from injury, surgical procedures, and underlying medical conditions, are a common medical condition, and wound care poses a major burden to the healthcare system in the US and worldwide[1,2]. A retrospective analysis of Medicare beneficiaries in the US for the 2014 calendar year determined that 14.5% of beneficiaries (8.2 million patients) were diagnosed with wounds, with or without infection, and that infected surgical wounds were the most common category (4.0% of beneficiaries) followed by infected diabetic wounds (3.4% of beneficiaries) and nonhealing surgical wounds (3.0% of beneficiaries). A conservative estimate of the cost of treatment for acute and chronic wounds was $31.7 billion; this estimate only reflects care received through the Medicare system, and the cost is expected to be substantially higher if patients using other payment systems are included[1].

Wound infections present a significant medical challenge, complicating healing and often leading to outcomes such as chronic wounds or systemic infections[3,4]. The rise of microbial resistance to antibiotics further exacerbates this problem, creating an urgent need for alternative strategies[5,6]. To that end, investigators have sought to expand the armamentarium of treatment options by repurposing existing drugs which have demonstrated antimicrobial activity[7], an approach that affords benefits such as faster regulatory approval and reduced costs[8]. Selective serotonin reuptake inhibitors (SSRIs), commonly used for the treatment of psychiatric disorders, have emerged as potential candidates[9–11], and recent work has established the minimum inhibitory concentrations (MICs) of the SSRI fluoxetine in combination with antibiotics against several clinically important species of bacteria[12–14].

Previously, we showed that fluoxetine reduced biofilm formation in *S. aureus* infected human ex-vivo wounds, and enhanced healing in *S. aureus* infected mouse excisional wounds[15]. In addition to potential antimicrobial effects, fluoxetine has been shown to have pro-reparative effects, improving skin wound healing[15–19]. Studies have demonstrated enhanced keratinocyte migration and neovascularization, reduced expression of inflammatory cytokines, and a shift in macrophage polarization towards a less inflammatory and more pro-reparative phenotype. For these reasons, we chose fluoxetine as the drug to be delivered in this study.

Recently developed endogenously responsive drug delivery systems (DDSs) are activated by signals from the wound, such as temperature[20–22] or chemical signals[23–26]. In such devices, the rate of drug release depends primarily on the characteristics of the encapsulating matrix[27]; in addition, physiological signals may not be sufficiently strong to trigger drug release at the appropriate time[28]. To remedy this, several groups have developed exogenously responsive drug delivery systems which provide greater control over the dose and timing of drug release. Systems have been designed to respond to the programmed application of electric fields[29], temperature[30], and light[31,32]. However, there is a need for devices which allow for highly precise and fully programmable control of drug delivery[28]. To this end, we developed a programmable, wirelessly controlled, wearable wound management device containing a voltage driven iontophoretic actuator for delivery of fluoxetine and an integrated high-resolution wound imaging system. The device is controlled remotely via wireless commands sent from a laptop, using a software module with a user-friendly graphical interface, and the treatment program is carried out in real-time.

The goal of the current work is to compare the pharmacokinetics of topically applied fluoxetine when delivered using the experimental device to conventional bolus pipette delivery. We hypothesize that topical delivery can produce effective concentrations of fluoxetine in the wound without systemic perturbation, and that metered delivery using the device will optimize absorption into the wound tissue. Using a porcine wound model, wound tissue concentrations were interrogated after topical bolus dosing or application using the device, and pharmacokinetic parameters of fluoxetine in the wound were established. To examine the potential for off-target effects, pig plasma was interrogated for systemic fluoxetine and norfluoxetine, and for changes in serotonin. In addition, we interrogated the wound tissues for serotonin to examine the ability of topical fluoxetine to modulate skin serotonin levels.

Device Design and Principles of Operation

The experimental device contains an iontophoresis pump actuator and wireless imaging module in a wearable format and is described in detail in our other work[33]. A schematic of the device is shown in Figure 1.

The actuator is voltage-driven, fully programmable, and allows for precise delivery of fluoxetine ions to the wound. The polydimethylsiloxane (PDMS) base contains reservoirs with microchannels for ion transport. Hydrogel ion exchange membranes are embedded within glass capillaries in the PDMS and serve as interfaces between the device and the wound, selectively delivering fluoxetine and preventing counterion transfer. Silver wires in the reservoirs connect to a custom-printed circuit board (PCB) for device control, described in our other work[34,35], and the circuit is completed by a counter electrode and the wound bed.

The PCB controls the applied voltage, V_{FLX}, which drives fluoxetine ions from the reservoir into the wound via the working electrode. The PCB also manages wireless communication to an external computer for real-time monitoring and data transmission. V_{FLX} is adjustable from zero to 4.7 V through a microcontroller and digital-to-analog converter (DAC).

The imaging module is a high-resolution camera positioned at the center of the PDMS actuator, and the clear bottom of the actuator serves as a lens. The camera captures images of the wound bed which are transmitted wirelessly to a computer, allowing for continuous monitoring of the wound. The actuator and camera are enclosed in a protective casing and affixed to a commercially available adhesive bandage.

The device supports wireless operation, and commands from a computer regulate both the ion pump and imaging processes. By combining targeted drug delivery with real-time monitoring, the device is designed to enhance wound healing in clinical and experimental settings.

Methods

Pig acclimation and wounding surgery

Yorkshire-Landrace-Duroc cross breed pigs (28-87 kg, 9-12 months old, female) were purchased from the UC Davis Swine Research Center. All animal work was approved by the UC Davis Institutional Animal Care and Use Committee (protocol #23353). Animals were acclimated for 7-10 days and trained for harness use and human contact as previously described[36]. Surgical preparation and wounding were as described[36], with the modification of prophylactic intravenous administration of Cefazolin, 30-35 mg/kg, during surgery. Baseline blood samples were collected and stored for plasma assays.

Six to ten circular wounds of 20 mm diameter and 6-10 mm depth were created on the paravertebral area of the pig as previously described[36], rinsed with 0.001% cefazolin solution, and dressed as previously described[36] for pipette and standard of care treatments, or with the experimental devices. The devices were connected to a V75 battery (Voltaic Systems, New York, USA) and Raspberry Pi 4B controller (Raspberry Pi Ltd., Cambridge, England), carried in 2 Molle pouches (Tacticool Firearms, Virginia, USA) attached to the shoulder harness of the pig. The post-operative analgesic buprenorphine, 0.005-0.01 mg/kg, was given by intramuscular injection before extubation, and a fentanyl patch was applied at the end of surgery. Pigs were monitored for signs of hyperthermia after recovery.

Fabrication of the Wearable PDMS Device

The PDMS actuator contains three main components which were molded separately: the reservoir, the notch, and the channel piece. The molds were 3D printed using a Formlabs 3B printer with Model V3 resin at a layer thickness of 50 um. To improve optical performance, an additional mold was made from CNC-milled acrylic disks with a 19.5 mm diameter.

PDMS (Sylgard 184) base and cross-linker were mixed in a 10:1 ratio. The mixture was degassed, poured into the molds, leveled, and degassed again. The molds were cured at 60°C for 48 hours. Once cured, the PDMS components were cleaned in isopropanol (IPA), rinsed with water, and oven-dried for assembly.

Silver wires were inserted into the PDMS reservoirs, and PDMS seals were applied at the insertion points to prevent leaks. The device was assembled using plasma bonding; surfaces were exposed to plasma for 10 seconds and then cured for 30 minutes at 60°C. Bond quality was tested by injecting air into the reservoirs.

Adhesive tape was applied to protect the optical window, and parylene coating was performed over the course of three hours to produce a durable protective layer. The PCB was attached to the top of the PDMS, electrodes were soldered to the corresponding pins on the PCB, and a chlorinated silver wire was attached to serve as the counter electrode. A second parylene layer was applied for additional protection.

Preparation of the Hydrogel Capillaries

Glass capillaries of 0.800 mm internal diameter were cleaned with NaOH and conditioned with deionized water, silane coupling agent, and ethanol. Once dry, the capillaries were filled with a hydrogel precursor and UV-cured at 7 mW/cm². The cured hydrogel was cut into 5 mm segments and soaked in fluoxetine solution.

Capillary Insertion and Final Assembly

The device and capillaries were sterilized in a biosafety cabinet using UV radiation for 30 minutes, and the remaining steps were performed in a biosafety cabinet using aseptic technique.

The capillary segments were inserted into the actuator channels using a biopsy punch, and the reservoirs were filled with fluoxetine solution. The channels were sealed using 3D-printed biocompatible caps. The assembled device was mounted onto a New Image Flat CeraPlus Skin Barrier (Hollister, Illinois, USA) for attachment to the wound site, and the finished devices were placed into autoclaved steel bins for transport to the surgery room.

Device Startup and Daily Operation

Upon startup, the device entered standby mode and connected to a designated Wi-Fi network in the vivarium. Researchers controlled the device remotely via wireless commands sent from a laptop, using a software module with a user-friendly graphical interface. The laptop also ran software modules for wound stage prediction[37] and closed loop control using a machine-learning algorithm[38], which were tested in a different set of pig experiments.

The device operated for 22 hours daily with a 2-hour standby window for data transfer, battery replacement, and routine checks. The battery supported up to 36 hours of operation and was replaced daily. After each battery change the device data were copied to the laptop's hard drive, and the software module was manually reset. This was repeated daily during the experiment.

Fluoxetine Delivery

Experimental devices were examined daily, and devices were replaced every 3-4 days during the experiments. Devices were programmed to deliver a target dose of 0.45 mg/wound/day within a six-, twelve-, or twenty-two hour treatment window. The actual dose delivered was calculated using current measurements recorded by the device controller. The actuator was programmed to stop automatically when the treatment target was reached or when the preset duration ended.

Wounds that received bolus topical fluoxetine solution, bolus saline control solution, or standard of care were examined daily, and dressings were replaced every 3-4 days or as needed. Sterile fluoxetine hydrochloride solution was prepared in saline and applied in doses of 0.45 mg/wound ('high' dose) or 0.025 mg/wound ('low' dose) on each day of application.

At the end of observation on post-operative days 3, 7, 10, or 22 (for device experiments) or on days 7 or 10 (for pipette experiments), plasma was collected, and the animal was euthanized. Wound tissue was excised with a 10 mm margin of surrounding intact skin, divided for HPLC, and flash-frozen using liquid nitrogen. Wound tissue was stored at -80°C until use.

Chromatographic Analysis of Fluoxetine and Norfluoxetine

Measurements were performed using reverse phase HPLC with UV absorbance detection. The system was a Neurotransmitters Analyzer (Antec Scientific, Leyden, Netherlands) coupled to a BlueShadow 40D detector (Knauer, Berlin, Germany). Separation was performed on an Acquity UPLC BEH C18 column (3.0 mm ID x 100 mm L, 1.7 um particles, Waters, Ireland) at a flow rate of 0.450 mL per minute and column oven temperature of 35°C. The mobile phase consisted of 35:65 acetonitrile: 45 mM phosphate buffer pH = 6.0, and column effluent was monitored at 230 nm.

Chromatographic Analysis of Serotonin

For serotonin analysis in the plasma, measurements were performed using reverse phase HPLC with UV absorbance detection. The system was an Antec Neurotransmitters Analyzer coupled to a Knauer BlueShadow 40D detector. Separation was performed on a Waters Acquity UPLC BEH C18 column (3.0 mm ID x 100 mm L, 1.7 um particles) at a flow rate of 0.450 mL per minute and column oven temperature of 37°C. The mobile phase consisted of 4:96 acetonitrile: 50 mM citrate buffer pH = 4.3, and column effluent was monitored at 275 nm.

For serotonin analysis in the pig wound tissues, measurements were performed using HPLC with electrochemical detection. The system was an Antec Neurotransmitters Analyzer fitted with a 2 mm glassy carbon working electrode and Ag/AgCl reference electrode (SenCell, Antec Scientific), operated in the DC mode at a potential of 0.460 V versus Ag/AgCl. Separation

was performed on a Waters Acquity UPLC BEH C18 column (1.0 mm ID x 100 mm L, 1.7 um particles) at a flow rate of 0.050 mL per minute and column oven temperature of 37°C. The mobile phase consisted of 4:96 acetonitrile: 50 mM citrate buffer pH = 4.3.

Extraction of Fluoxetine and Norfluoxetine from Pig Plasma
Pig plasma samples were purified on C18 solid-phase extraction (SPE) cartridges packed into glass tubes with glass fiber frits (Macherey-Nagel, Duren, Germany). Plasma extraction was carried out as follows: on a vacuum manifold, cartridges were conditioned with two tube volumes methanol and one tube volume water. Pig plasma (0.500 mL) was spiked with 50.0 uL internal standard solution (40.0 ug/mL fluvoxamine in methanol), diluted with 0.500 mL H_2O, and passed through the conditioned SPE cartridges. Next, cartridges were rinsed with one tube volume H2O followed by one tube volume 50:50 methanol: H_2O. Fluoxetine and norfluoxetine were eluted from the cartridges in 0.500 mL methanol containing 0.5% (v/v) formic acid, the eluate was made up to 1.000 mL by addition of 0.500 mL H_2O, and 10 uL was injected for analysis.

Extraction of Serotonin from Pig Plasma
Pig plasma samples were depleted of protein as follows: pig plasma (0.100 mL) was spiked with 5.00 uL antioxidant solution (1.3% (m/v) ascorbic acid and 2 mM EDTA in H_2O) and 20.00 uL internal standard solution (300.0 uM N-methylserotonin in H_2O). Next, 5.64 uL of 70% perchloric acid solution (Thermo Scientific, Waltham, Massachusetts) was added and the samples were vortexed for 30 seconds. The samples were centrifuged, and 10 uL of the supernatant was injected for analysis.

Tissue Cryo-pulverization
Pig wound tissues were briefly thawed and trimmed to a 2 mm margin of healthy skin at the wound edges. Fat was trimmed from the bottom of the tissue pieces, and large wounds were bisected. Tissues were diced using a razor blade, were immediately refrozen, and were crushed in a stainless-steel die (BioSpec Products, Bartlesville, Oklahoma) over liquid nitrogen. Using a porcelain mortar and pestle over liquid nitrogen, the crushed tissues were ground to the consistency of a fine powder. Frozen ground tissue was stored at -80°C until analysis.

Extraction of Fluoxetine and Norfluoxetine from Pig Wound Tissues
Ground pig wound tissues (20.0 to 30.0 mg) were resuspended in 0.250 mL methanol containing 0.5% (v/v) formic acid and 2.000 ug/mL fluvoxamine. The resuspended tissues were sonicated for 15 minutes in a sonicating bath, and the resulting tissue homogenates were centrifuged. The supernatants were transferred to clean microcentrifuge tubes and made up to 0.500 mL by addition of 0.250 mL H_2O, and 10 uL of this was injected for analysis.

Extraction of Serotonin from Pig Wound Tissues
Ground pig wound tissues (20.0 to 30.0 mg) were resuspended in 10 uL of 0.1 N $HClO_4$ per mg tissue and sonicated for 10 minutes in a sonicating bath. The resulting tissue homogenates were centrifuged, passed through 0.2 um nylon syringe filters (Thermo Scientific, Waltham, Massachusetts), loaded into pre-rinsed 30 kDa ultrafiltration cartridges (Pierce, Thermo Scientific) and centrifuged at 15,000 x G for 30 minutes. 3 uL of the filtrate was injected for analysis.

Statistical Analysis
Statistical analyses were performed in GraphPad Prism 10.2 software. Linear correlations were evaluated using Spearman's test for nonparametric data, and hypothesis testing for the comparison of regression lines was performed using ANCOVA. Test results of $p \leq 0.05$ were considered statistically significant. Outliers were identified using the ROUT function in Prism 10.2 software with a false discovery rate of Q = 2%.

Results

Fluoxetine delivery by the experimental device increases wound tissue concentrations compared to bolus pipette delivery
Pig wound tissue was collected after 3 or 7 days of daily topical fluoxetine application using either the experimental device or a pipette and was analyzed by HPLC to determine the fluoxetine tissue concentration. For both application modalities, the tissue level of fluoxetine was strongly correlated to the cumulative dose delivered (device, Spearman's R=0.862, p=0.0089; pipette, R=0.956, p=0.022). Norfluoxetine, the major active metabolite of fluoxetine, was not detected in any of the wound tissues (data not shown). Application using the fluoxetine device resulted in significantly higher absorption of fluoxetine into the wound tissues than bolus dosing using a pipette (p=0.0041, Figure 2).

Fluoxetine has a half-life of 0.99 days in the wound
After daily application of fluoxetine for 3 to 7 days using either the experimental device or a pipette (high- or low-dose), tissue was collected 1, 3, 4, 6, 8, or 16 days after the final application. The tissues were assayed for residual fluoxetine using HPLC, and the resulting concentrations are shown in Figure 3a. The pharmacokinetic parameters of fluoxetine in the wound tissue were determined according to the equation

$$C_T = C_0 \cdot e^{-kT} , \tag{1}$$

where C_T is the tissue concentration at time T, C_0 is the tissue concentration following the final dose, and k is the elimination constant. Rearranging this equation yields

$$\ln C_T = -kT + \ln C_0 , \tag{2}$$

which is a linear equation. Accordingly, the natural logarithms of the tissue concentrations were plotted against time, and the elimination constant k and the tissue concentration C_0 were determined graphically using the slope and y-intercept of the regression line[39] (Figure 3b). The half-life $T_{1/2}$ is the time required for one-half of the fluoxetine to be cleared from the wound tissue, such that

$$C_{T_{1/2}} = 0.5 \times C_0 , \tag{3}$$

and substituting into equation (1) yields

$$T_{1/2} = \frac{\ln(0.5)}{-k} . \tag{4}$$

The half-life of fluoxetine in the wound tissue was calculated for each dose regime and application modality, and the pharmacokinetic parameters are given in Table 1. The average half-life from the three conditions was 0.988 ± 0.256 days.

Topical fluoxetine is not absorbed into the systemic circulation

Fluoxetine was applied daily to two or four wounds, using either the experimental device or a pipette (high- or low-dose) for 3, 7, or 10 days, and plasma was collected one day after the final application. Plasma was analyzed for the presence fluoxetine and norfluoxetine, the primary active metabolite found in the blood of patients undergoing oral fluoxetine therapy. The limits of detection for our analysis were 7.4 ng/mL fluoxetine and 6.9 ng/mL norfluoxetine in pig plasma, and neither analyte was detected in the plasma after daily fluoxetine wound application (Figure 4).

Topical fluoxetine increases the serotonin concentration in the wound

Topical fluoxetine was applied daily for 7 days using the experimental device or a pipette, and wound tissue serotonin was measured one day after the final application. Tissue serotonin and fluoxetine levels were compared, and serotonin was found to be increased in the presence of intermediate, but not high, tissue concentrations of fluoxetine (Figure 5a and b).

Topical fluoxetine does not alter systemic serotonin

Fluoxetine was applied daily to two or four wounds using either the experimental device or a pipette (high- or low-dose) for 3, 7, or 10 days. The plasma serotonin concentration was measured prior to wounding and again one day after the final fluoxetine application, and the change in plasma serotonin, Δ serotonin, was calculated. For each pig, Δ serotonin was compared to the cumulative fluoxetine dose delivered to the animal to determine whether changes in plasma serotonin were related to the topical fluoxetine wound application (Figure 6). Δ Serotonin was not correlated with the duration of fluoxetine application or the cumulative fluoxetine dose administered to the pigs (3 days of dosing, Spearman's R=0.103, p=0.90; 7 days, R=0.200, p=0.917; 10 days, R=-1.00, p=0.33).

Discussion

Interest in fluoxetine as a repurposed therapeutic to expedite wound healing is growing. Pre-clinical studies have demonstrated multiple pro-reparative functions: enhanced keratinocyte migration and neovascularization, reduced inflammation, and a shift in macrophage polarization towards a pro-reparative phenotype[15–19]. More recently, fluoxetine has been investigated for its antibacterial properties[9,10]. Fluoxetine exhibits bactericidal activity against multidrug-resistant (MDR) clinical isolates of *A. baumannii, E. cloacae, E. coli, E. faecalis, E. faecium, K. pneumoniae*, and *S. aureus*, with minimum inhibitory concentrations (MICs) ranging from 32 to 512 ug/mL; furthermore, the addition of fluoxetine at 1 ug/mL dramatically reduced the MICs of ciprofloxacin against all the clinical isolates tested[12]. Fluoxetine was also found to be bactericidal against MDR clinical isolates of *E. coli* and *P. aeruginosa*, with MICs of 102 and 161 ug/mL, respectively; in addition, the MICs of erythromycin against the same clinical isolates were significantly reduced in the presence of fluoxetine at 1/8th of its MIC[13]. Most recently, fluoxetine was found to be bactericidal against several species of gram positive and gram negative bacteria,

with MICs of 64-128 ug/mL and 8-512 ug/mL, respectively, and that fluoxetine combined with polymyxin B produced synergistic killing against 80% of the gram-negative strains tested[14]. Here, we demonstrate that metered delivery of topical fluoxetine using the experimental device results in significantly increased tissue concentrations of fluoxetine compared to bolus dosing using a pipette. Crucially, the experimental device produced a maximum concentration of 12.25 ug fluoxetine/mL tissue, above the MIC for one strain of *A. baumanii* and sufficient to produce synergistic killing with antibiotics against several MDR strains of gram-positive and gram-negative bacteria. Furthermore, the tissue concentration of fluoxetine was strongly correlated to the cumulative dose administered using the experimental device, which should allow physicians to reliably produce therapeutic concentrations in the wound tissue.

Future iterations of the device have the potential for closed-loop, wound stage-specific treatments and could identify the four classical stages: hemostasis, inflammation, proliferation, and maturation[40,41]. Each stage entails a distinct set of cellular and biochemical processes, and traditional standardized wound care protocols may not adapt to the evolving state of the wound. Integrated closed-loop systems have been developed to initiate treatment in real-time in response to wound assessments[28]; however, so far, no closed-loop devices exist to deliver adaptive treatments based on the wound stage[28]. To address this need, we developed a closed-loop system which supports AI-driven monitoring and decision making. The integrated camera within the device captures high-resolution images of the wound at regular intervals and transmits them to a central server, where they are processed by two models: a stage-evaluation AI model and a decision-making deep reinforcement leaning model (DRL). The models evaluate the wound stage and create a revised treatment plan which is transmitted to the device controller and implemented in real-time. More information about the closed loop functionality of the device is described in our other work[33].

The pharmacokinetics of fluoxetine as an oral therapy for psychiatric conditions have been well studied since the 1970's[42]. Fluoxetine is lipophilic and has a large volume of distribution (V_d), indicating extensive accumulation in tissues[43–45]. For this reason, fluoxetine has a long elimination half-life of 1-4 days[44,46]. However, the pharmacokinetics of fluoxetine in wound skin are not well understood. Transdermal delivery systems have been developed[47–49] but, due to the barrier function of the intact epidermis, these studies provide limited insight into the pharmacokinetics of fluoxetine in wounds where the epidermis is not present and delivered drug has access to the dermal vasculature. In addition, although some groups used carriers to increase tissue absorption, skin fluoxetine levels were not measured. We found that fluoxetine had a half-life of 0.988 ± 0.256 days in the wound tissue, consistent with the elimination half-life measured in the blood after oral dosing[44,46]. Determination of the half-life of fluoxetine in wound tissue may inform the frequency of topical application. Once-daily oral dosing with fluoxetine is often used for the treatment of psychiatric conditions[50], and this also may be suitable for fluoxetine topical wound therapy. In multiple-dosing, a fixed dose is applied repeatedly at intervals of one half-life; typically, steady state concentrations occur after 5 doses and are twice the concentration achieved after the initial dose[39]. If fluoxetine is applied too infrequently a therapeutic concentration may not be achieved, while accumulation to higher than desirable levels can occur if application is too frequent[39]. Thus, the advantage of the experimental device described here is that its programmable dosing can be adjusted to deliver fluoxetine at precise intervals, offering an advantage over manual dosing where accurate timing of each dose may be a challenge. In addition, automated dosing from the device may simplify wound treatment and improve patient adherence to the treatment regimen.

Fluoxetine is considered to have a good safety profile[51,52], exhibiting high specificity for serotonin uptake sites and low affinity for serotonin receptors and the uptake sites of norepinephrine[53] and dopamine[54]. Common side effects are limited and life threatening side effects such as cardiotoxicity and CNS toxicity are rare due to the lack of monoamine receptor antagonism[44]. In addition, drug-drug interactions are possible and have become important selection criteria when considering fluoxetine use[55,56]. Fluoxetine inhibits the isoenzymes CYP2D6[57–59] and, to a lesser extent, CYP3A3/4[60] and produces impairments in the clearance of drugs metabolized by these cytochromes, such as TCAs, neuroleptics, alprazolam, and carbamazepine[44]. Due to the possibility of side effects and drug-drug interactions, we evaluated systemic absorption of fluoxetine after topical administration to the wound bed, by analyzing plasma levels of fluoxetine and its metabolite norfluoxetine after application to porcine skin wounds. Fluoxetine and norfluoxetine were not detectable in the plasma after 3, 7, or 10 days of daily topical wound application. The therapeutic window for the combined concentration of fluoxetine and norfluoxetine in the blood of patients undergoing oral fluoxetine therapy is 120 to 500 ng/mL[61], and the results of the present study suggest that side effects and drug-drug interactions are unlikely to result from topical application of fluoxetine to wounds.

When fluoxetine is used as a topical therapy for wounds, effects should ideally occur only in the wound site. Fluoxetine has the potential to alter systemic serotonin levels. Plasma serotonin increases (~60%) shortly after oral fluoxetine administration (7 to 10 hours)[62], but then decreases after long term (8 weeks) daily treatment[63]. To investigate the possibility of unwanted systemic effects in the experimental animals, plasma serotonin was measured prior to each experiment and again at the experimental endpoint. We found that changes in plasma serotonin levels were not correlated with the cumulative doses of fluoxetine delivered to the animals on their wounds. Taken together with the lack of detectable fluoxetine and norfluoxetine in the plasma, these results indicate that topical fluoxetine wound treatment is unlikely to produce systemic effects.

Fluoxetine is thought to improve skin wound healing through the modulation of serotonin signaling. The primary source of serotonin in the skin is in platelets, but serotonin is also synthesized and stored in skin cells[64–66]. Serotonergic neurons are not present in the skin[64]. Fluoxetine prevents cellular reuptake by blocking the serotonin transporter SERT, which is expressed on immune cells[65], keratinocytes[67,68], fibroblast[69], and Merkel cells[66]; SERT is also expressed on platelets, and fluoxetine has been shown to reduce the platelet-bound fraction of serotonin in the blood[70,71]. It follows that fluoxetine may increase extracellular serotonin in the wound skin. Serotonin receptors comprise a family of G protein-coupled and ligand-gated ion channel receptors expressed on cell surfaces[72], and an increase in unsequestered serotonin may enhance signaling and produce beneficial effects on healing. In in-vivo scratch wound models using primary human keratinocytes, serotonin accelerated closure in a dose dependent manner[16,69], and other groups have found that serotonin skewed human macrophage polarization towards a less inflammatory phenotype[73] and reduced the expression of the pro-inflammatory cytokines TNFa and IL6[74]. Fluoxetine treatment produced similar effects in an excisional wound model using diabetic mice, enhancing re-epithelialization, reducing the expression of TNFa and IL6, and shifting macrophage polarization towards a less inflammatory and more pro-reparative phenotype[16]. Here, we report for the first time the serotonin modulating effects of fluoxetine in the skin, where fluoxetine at intermediate, but not high, tissue concentrations increased the total tissue level of serotonin. This suggests that in the case of non-infected wounds, lower tissue concentrations of fluoxetine may be more beneficial for healing. However, more work is needed

to investigate changes in the proportions of free and sequestered serotonin in the wound tissue independent of changes in the total amount. A key advantage of the experimental device is programmable dosing which can be adjusted depending on the specific use case; higher doses can be applied to elicit an antimicrobial effect in the case of infected wounds, and lower doses can be delivered to stimulate healing by modulation of tissue serotonin in the case of uninfected wounds.

Conclusion

In this study, we demonstrated that a bioelectronic wound treatment device can effectively deliver topical fluoxetine to wounds with minimal risk of off-target effects. The experimental device produces higher tissue concentrations of fluoxetine at lower cumulative doses compared to bolus dosing, which may lead to greater efficacy when fluoxetine is used as an adjunctive therapy for infected wounds. We established basic pharmacokinetic parameters of fluoxetine in the wound tissue and investigated the effects of fluoxetine on the endogenous serotonin system in the skin. The device may simplify wound treatment by reducing the burden for daily drug application, possibly increasing adherence to a prescribed treatment regimen. Recent iterations of the device incorporate closed-loop feedback control using integrated imaging and machine learning to produce real-time adaptive treatments based on the predicted wound stage, and work is ongoing to optimize the design for commercialization and clinical use.

Author Contributions

Anthony Gallegos: Writing – original draft; writing – review and editing; conceptualization; investigation; methodology; formal analysis. **Houpu Li:** Writing – review and editing; investigation; methodology; software. **Hsin-ya Yang:** Writing – review and editing; investigation; methodology. **Guillermo Villa-Martinez:** Investigation; methodology. **Itidal Bazzi:** Investigation. **Samhitha Sathyanarayanan:** Investigation. **Narges Asefifeyzabadi:** Investigation; software. **Prabhat Baniya:** Methodology; software. **Wan Shen Hee:** Investigation; software. **Mo Siadat:** Investigation. **Elizabeth Chang:** Investigation. **Sriansh Pasumarthi:** Investigation. **Mircea Teodorescu:** Conceptualization; methodology; resources; funding acquisition. **Marcella Gomez:** Conceptualization; software; methodology; funding acquisition. **Marco Rolandi:** Supervision; conceptualization; methodology; resources; funding acquisition; writing – review and editing. **Rivkah Isseroff:** Supervision; conceptualization; methodology; resources; funding acquisition; writing – review and editing.

Acknowledgements

This research is sponsored by the Defense Advanced Research Projects Agency (DARPA) and the Advanced Research Projects Agency for Health (ARPA-H) through Cooperative Agreement D20AC00003 awarded by the US Department of the Interior (DOI), Interior Business Center. The content of the information does not necessarily reflect the position or the policy of the government, and no official endorsement should be inferred.

We thank Justine Arizabal for creating the wound illustrations used in this paper.

Conflict of Interest Statement

The authors have no conflicts of interest to declare.

Data Availability Statement
Data supporting this study are available from the corresponding author upon reasonable request.

OrcId
Anthony Gallegos https://orcid.org/my-orcid?orcid=0000-0003-1667-9065

References

1. Nussbaum S, Carter M, Fife C, et al. An economic evaluation of the impact, cost, and medicare policy implications of chronic non-healing wounds. *Value Health*. 2018;21(1):27-32.

2. Sen C. Human wounds and its burden: an updated compendium of estimates. *Adv Wound Care (New Rochelle)*. 2019;8(2):39-48.

3. Williams H, Campbell L, Crompton R, et al. Microbial host interactions and impaired wound healing in mice and humans: defining a role for BD14 and NOD2. *J Invest Dermatol*. 2018;138(10):2264-2274.

4. Zhao R, Liang H, Clarke E, Jackson C, Xue M. Inflammation in chronic wounds. *Int J Mol Sci*. 2016;17(12):2085.

5. Hansson K, Brenthel A. Imagining a post-antibiotic era: a cultural analysis of crisis and antibiotic resistance. *Med Humanit*. 2022;48(3):381-388.

6. Spellberg B, Bartlett J, Wunderink R, Gilbert D. Novel approaches are needed to develop tomorrow's antibacterial therapies. *Am J Respir Crit Care Med*. 2014;191(2):135-140.

7. Foletto V, da Rosa T, Serafin M, Bottega A, Horner R. Repositioning of non-antibiotic drugs as an alternative to microbial resistance: a systematic review. *Int J Antimicrob Agents*. 2021;58(3):106380.

8. Begley CG, Ashton M, Baell J, et al. Drug repurposing: misconceptions, challenges, and opportunities for academic researchers. *Sci Transl Med*. 2021;13(612):eabd5524.

9. Munoz-Bellido JL, Munoz-Criado S, Garcia-Rodriguez JA. Antimicrobial activity of psychotropic drugs Selective serotonin reuptake inhibitors. *Int J Antimicrob Agents*. 2000;14(3):177-180.

10. Racz B, Spengler G. Repurposing antidepressants and phenothiazine antipsychotics as efflux pump inhibitors in cancer and infectious diseases. *Antibiotics (Basel)*. 2023;12(1):137.

11. Koh Jing Jie A, Hussein M, Rao G, Li J, Velkov T. Drug repurposing approaches toward defeating multidrug-resistant gram-negative pathogens: novel polymixin/non-antibiotic combinations. *Pathogens*. 2022;11(12):1420.

12. Foletto V, da Rosa T, Serafin M, et al. Repositioning of antidepressant drugs and synergistic effect with ciprofloxacin against multidrug-resistant bacteria. *World J Microbiol Biotechnol*. 2021;37(3):53.

13. Karine de Sousa A, Rocha JE, Goncalves de Souza T, Sampaio de Freitas T, Ribeiro-Filho J, Melo Coutinho HD. New roles of fluoxetine in pharmacology: antibacterial effect and modulation of antibiotic acitivity. *Microb Pathog*. 2018;123:368-371.

14. Ahmed S, Jordan R, Isseroff RR, Lenhard J. Potential synergy of fluoxetine and antibacterial agents against skin and soft tissue pathogens and drug-resistant organisms. *Atibiotics*. 2024;13(12):1165.

15. Yoon D, Nguyen C, Bagood M, et al. Topical fluoxetine as a potential nonantibiotic adjunctive therapy for infected wounds. *J Invest Dermatol*. 2021;141(6):1608-1612.

16. Nguyen C, Tartar D, Bagood M, et al. Topical fluoxetine as a novel therapeutic that improves wound healing in diabetic mice. *Diabetes*. 2019;68(7):1499-1507.

17. Farahani RM, Sadr K, Rad JS, Mesgari M. Fluoxetine enhances cutaneous wound healing in chronically stressed wistar rats. *Adv Skin Wound Care*. 2007;20(3):157-165.

18. Fatima F, Aleemuddin M, Ahmed MM, et al. Design and evaluation of solid lipid nanoparticles loaded topical gels: repurpose of fluoxetine in diabetic wound healing. *Gels*. 2022;9(1):21.

19. Rodriguez-Barucg Q, Garcia A, Garcia-Merino B, et al. Environmental fluoxetine promotes skin cell proliferation and wound healing. *Environ Pollut*. 2024;362:124952.

20. Gao B, Guo M, Lyu K, Chu T, He B. Intelligent silk fibroin based microneedle dressing (i-SMD). *Advanced Functional Materials*. 2021;31(3):2006839. doi:10.1002/adfm.202006839

21. Van Gheluwe L, Chourpa I, Gaigne C, Munnier E. Polymer-based smart drug delivery systems for skin application and demonstration of stimuli-responsiveness. *Polymers (Basel)*. 2021;13(8):1285. doi:10.3390/polym13081285

22. Liu J, Chen Z, Wang J, et al. Encapsulation of curcumin nanoparticles with MMP9-responsive and thermos-sensitive hydrogel improves diabetic wound healing. *ACS Appl Mater Interfaces*. 2018;10(19):16315-16326. doi:10.1021/acsami.8b03868

23. Zhao L, Niu L, Liang H, Tan H, Liu C, Zhu F. pH and glucose dual-responsive injectable hydrogels with insulin and fibroblasts as bioactive dressings for diabetic wound healing. *ACS Appl Mater Interfaces*. 2017;9(43):37563-37574. doi:10.1021/acsami.7b09395

24. Hu C, Zhang F, Long L, Kong Q, Luo R, Wang Y. Dual-responsive injectable hydrogels encapsulating drug-loaded micelles for on-demand antimicrobial activity and accelerated wound healing. *J Control Release*. 2020;324:204-217. doi:10.1016/j.jconrel.2020.05.010

25. Yao Q, Kou L, Tu Y, Zhu L. MMP-responsive “smart” drug delivery and tumor targeting. *Trends Pharmacol Sci*. 2018;39(8):766-781. doi:10.1016/j.tips.2018.06.003

26. Chen H, Qin Z, Zhao J, et al. Cartilage-targeting and dual MMP-13/pH responsive theranostic nanoprobes for osteoarthritis imaging and precision therapy. *Biomaterials*. 2019;225:119520. doi:10.1016/j.biomaterials.2019.119520

27. Timko BP, Dvir T, Kohane DS. Remotely triggerable drug delivery systems. *Adv Mater*. 2010;22(44):4925-4943. doi:10.1002/adma.201002072

28. Wang C, Sani ES, Gao W. Wearable bioelectronics for chronic wound management. *Adv Funct Mater*. 2022;32(17):2111022. doi:10.1002/adfm.202111022

29. Kiaee G, Mostafalu P, Samandari M, Sonkusale S. A pH-mediated electronic wound dressing for controlled drug delivery. *Adv Healthc Mater*. 2018;7(18):e1800396. doi:10.1002/adhm.201800396

30. Mostafalu P, Kiaee G, Giatsidis G, et al. A textile dressing for temporal and dosage controlled drug delivery. *Advanced Functional Materials*. 2017;27(41):1702399. doi:10.1002/adfm.201702399

31. Zhao X, Liu Y, Shao C, et al. Photoresponsive delivery microcarriers for tissue defects repair. *Adv Sci (Weinh)*. 2019;6(20):1901280. doi:10.1002/advs.201901280

32. Chen H, Cheng Y, Tian J, et al. Dissolved oxygen from microalgae-gel patch promotes chronic wound healing in diabetes. *Sci Adv*. 2020;6(20):eaba4311. doi:10.1126/sciadv.aba4311

33. Li H, Yang H, Lu F, et al. Real-time diagnostics and personalized wound therapy powered by AI and bioelectronics. Published online January 13, 2025:2025.01.12.25320338. doi:10.1101/2025.01.12.25320338

34. Li H, Asefifeyzabadi N, Schorger K, et al. Remote-controlled wireless bioelectronics for fluoxetine therapy to promote wound healing in a porcine model. Published online December 21, 2024:2024.12.18.629272. doi:10.1101/2024.12.18.629272

35. Baniya P, Tebyani M, Hee WS, et al. Wireless bioelectronic device for wound healing. Published online December 20, 2024:2024.12.18.629068. doi:10.1101/2024.12.18.629068

36. Yang H, Fierro F, Yoon D, et al. Combination product of dermal matrix, preconditioned human mesenchymal stem cells and timolol promotes healing in the porcine wound model. *J Biomed Mater Res B Appl Biomater*. 2022;110(7):1615-1623.

37. Lu F, Zlobina K, Osorio S, et al. DeepMapper: attention-based autoencoder for system identification in wound healing and stage prediction. Published online December 20, 2024:2024.12.17.628977. doi:10.1101/2024.12.17.628977

38. Lu F, Zlobina K, Baniya P, et al. Accelerating wound healing through deep reinforcement learning: a data-driven approach to optimal treatment. Published online December 21, 2024:2024.12.18.629218. doi:10.1101/2024.12.18.629218

39. Kenakin TP. Chapter 9: Pharmacokinetics. In: Kenakin TP, ed. *A Pharmacology Primer*. 5th ed. Academic Press; 2019:245-293.

40. Gurtner G, Werner S, Barrandon Y, Longaker M. Wound repair and regeneration. *Nature*. 2008;453(7193):314-321.

41. Rodrigues M, Kosaric N, Bonham C, Gurtner G. Wound healing: a cellular perspective. *Physiol Rev*. 2019;99(1):665-706.

42. Wong D, Perry K, Bymaster F. The discovery of fluoxetine hydrochloride (prozac). *Nat Rev Drug Discov*. 2005;4(9):764-774.

43. Gram L. Fluoxetine. *N Engl J Med*. 1994;331(20):1354-1361. doi:10.1056/NEJM199411173312008

44. Hiemke C, Hartter S. Pharmacokinetics of selective serotonin reuptake inhibitors. *Pharmacol Ther*. 2000;85(1):11-28.

45. Catterson ML, Preskorn SH. Pharmacokinetics of selective serotonin reuptake inhibitors: clinical relevance. *Pharmacol Toxicol*. 1996;78(4):203-208. doi:10.1111/j.1600-0773.1996.tb00206.x

46. Altamura AC, Moro AR, Percudani M. Clinical pharmacokinetics of fluoxetine. *Clin Pharmacokinet*. 1994;26(3):201-214. doi:10.2165/00003088-199426030-00004

47. Ciribassi J, Luescher A, Pasloske KS, Robertson-Plouch C, Zimmerman A, Kaloostian-Whittymore L. Comparative bioavailability of fluoxetine after transdermal and oral administration to healthy cats. *Am J Vet Res*. 2003;64(8):994-998. doi:10.2460/ajvr.2003.64.994

48. Jung E, Kang YP, Yoon IS, et al. Effect of permeation enhancers on transdermal delivery of fluoxetine: in vitro and in vivo evaluation. *Int J Pharm*. 2013;456(2):362-369. doi:10.1016/j.ijpharm.2013.08.080

49. Parikh DK, Ghosh TK. Feasibility of transdermal delivery of fluoxetine. *AAPS PharmSciTech*. 2005;6(2):E144-149. doi:10.1208/pt060222

50. Prozac (Fluoxetine Hydrochloride) Prescribing Information. Eli Lilly and Company, Indeapnapolis, IN 46285, USA. Accessed December 23, 2024. https://www.accessdata.fda.gov/drugsatfda_docs/label/2011/018936s091lbl.pdf

51. de Jonghe F, Swinkels JA. The safety of antidepressants. *Drugs*. 1992;43 Suppl 2:40-46; discussion 46-47. doi:10.2165/00003495-199200432-00007

52. Abu Assab M, Lewis G, Normand C. Are SSRIs a cost-effective alternative to tricyclics? *Br J Psychiatry*. 1996;168(4):404-409. doi:10.1192/bjp.168.4.404

53. Frazer A. Pharmacology of antidepressants. *J Clin Psychopharmacol*. 1997;17(2):2s-18s.

54. Stanford SC. Prozac: panacea or puzzle? *Trends Pharmacol Sci*. 1996;17(4):150-154. doi:10.1016/0165-6147(96)81591-4

55. Baumann P. Pharmacology and pharmacokinetics of citalopram and other SSRIs. *Int Clin Psychopharmacol*. 1996;11 Suppl 1:5-11. doi:10.1097/00004850-199603001-00002

56. Van den Berg SJ. Comparing SSRIs: From chemistry to clinical choice. *Hum Psychopharmacol*. 1995;10 Suppl 3(S3):S199-S209. doi:10.1002/hup.470100909

57. Bergstrom RF, Peyton AL, Lemberger L. Quantification and mechanism of the fluoxetine and tricyclic antidepressant interaction. *Clin Pharmacol Ther*. 1992;51(3):239-248. doi:10.1038/clpt.1992.18

58. Stevens JC, Wrighton SA. Interaction of the enantiomers of fluoxetine and norfluoxetine with human liver cytochromes P450. *J Pharmacol Exp Ther*. 1993;266(2):964-971.

59. Otton SV, Wu D, Joffe RT, Cheung SW, Sellers EM. Inhibition by fluoxetine of cytochrome P450 2D6 activity. *Clin Pharmacol Ther*. 1993;53(4):401-409. doi:10.1038/clpt.1993.43

60. Greenblatt DJ, von Moltke LL, Schmider J, Harmatz JS, Shader RI. Inhibition of human cytochrome P450-3A isoforms by fluoxetine and norfluoxetine: in vitro and in vivo studies. *J Clin Pharmacol*. 1996;36(9):792-798. doi:10.1002/j.1552-4604.1996.tb04252.x

61. FLUOX - Overview: Fluoxetine, Serum. Accessed December 5, 2024. https://www.mayocliniclabs.com/test-catalog/overview/80228#Clinical-and-Interpretive

62. Blardi P, De Lalla A, Leo A, et al. Serotonin and fluoxetine levels in plasma and platelets after fluoxetine treatment in depressive patients. *J Clin Psychopharmacol*. 2002;22(2):131-136.

63. Holck A, Wolkowitz O, Mellon S, et al. Plasma serotonin levels are associated with antidepressant response to SSRIs. *J Affect Disord*. 2019;250:65-70.

64. Johansson O, Liu PY, Bondesson L, et al. A serotonin-like immunoreactivity is present in human cutaneous melanocytes. *J Invest Dermatol*. 1998;111(6):1010-1014. doi:10.1046/j.1523-1747.1998.00460.x

65. Ahern GP. 5-HT and the immune system. *Curr Opin Pharmacol*. 2011;11(1):29-33. doi:10.1016/j.coph.2011.02.004

66. Nordlind K, Azmitia EC, Slominski A. The skin as a mirror of the soul: exploring the possible roles of serotonin. *Experimental Dermatology*. 2008;17(4):301-311. doi:10.1111/j.1600-0625.2007.00670.x

67. Thorslund K, El-Nour H, Nordlind K. The serotonin transporter protein is expressed in psoriasis, where it may play a role in regulating apoptosis. *Arch Dermatol Res*. 2009;301(6):449-457. doi:10.1007/s00403-009-0933-y

68. Zabolinejad N, Molkara S, Bakhshodeh B, Ghaffari-Nazari H, Khoshkhui M. The expression of serotonin transporter protein in the skin of patients with chronic spontaneous urticaria and its relation with depression and anxiety. *Arch Dermatol Res*. 2019;311(10):825-831. doi:10.1007/s00403-019-01969-y

69. Sadiq A, Shah A, Jeschke M, et al. The role of serotonin during skin healing in post-thermal injury. *Int J Mol Sci*. 2018;19(4):1034.

70. Lemberger L, Rowe H, Carmichael R, et al. Pharmacologic effects in man of a specific serotonin-reuptake inhibitor. *Science*. 1978;199(4327):436-437. doi:10.1126/science.619465

71. Horng JS, Wong DT. Effects of serotonin uptake inhibitor, Lilly 110140, on transport of serotonin in rat and human blood platelets. *Biochem Pharmacol*. 1976;25(7):865-867. doi:10.1016/0006-2952(76)90162-3

72. Kitson SL. 5-hydroxytryptamine (5-HT) receptor ligands. *Curr Pharm Des*. 2007;13(25):2621-2637. doi:10.2174/138161207781663000

73. de las Casas-Engel M, Dominguez-Soto A, Sierra-Filardi E, et al. Serotonin skews human macrophage polarization through HTR2b and HTR7. *J Immunol*. 2013;190(5):2301-2310.

74. Kubera M, Maes M, Kenis G, Kim YK, Lasoń W. Effects of serotonin and serotonergic agonists and antagonists on the production of tumor necrosis factor α and interleukin-6. *Psychiatry Res*. 2005;134(3):251-258. doi:10.1016/j.psychres.2004.01.014

Graphical Abstract

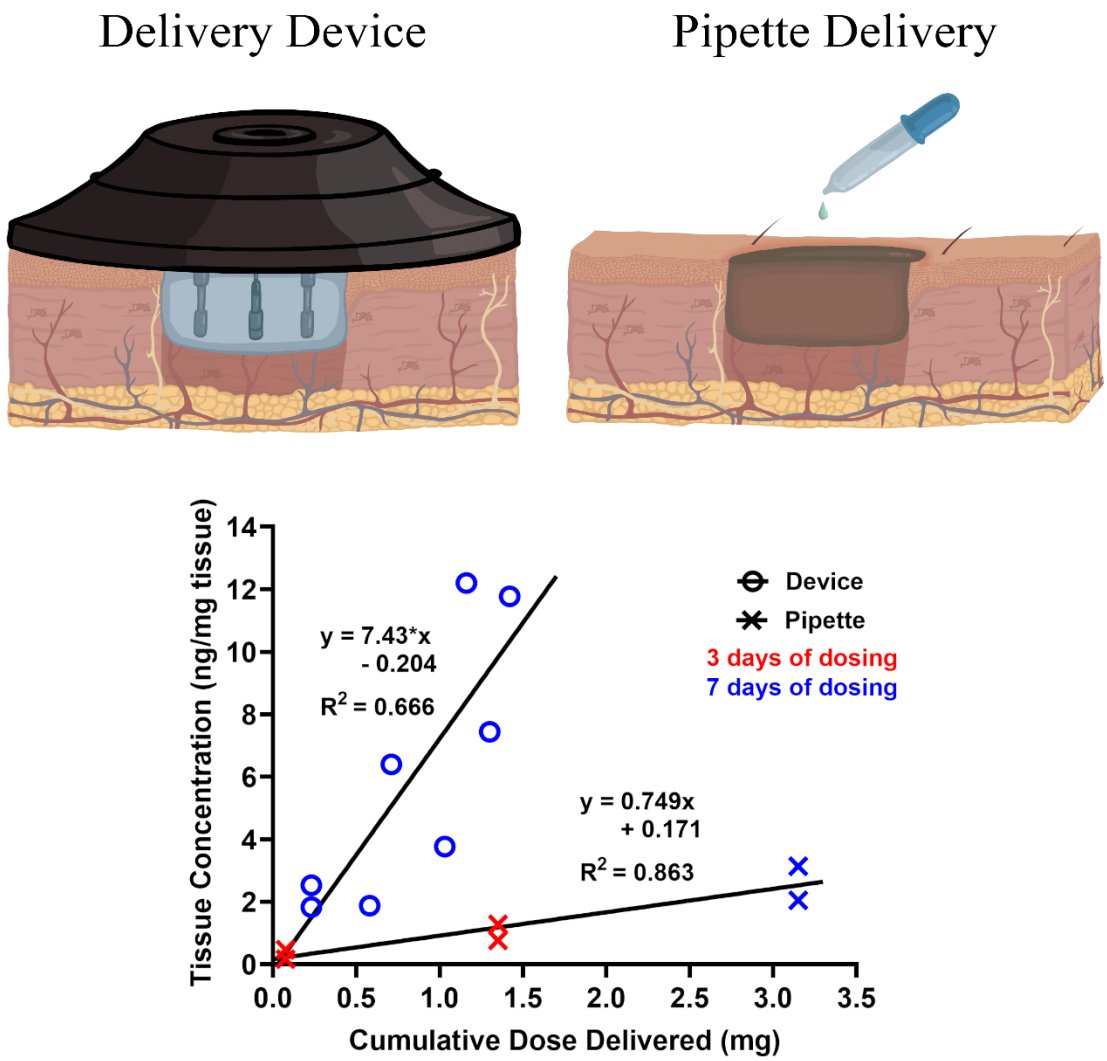

Figures and Figure Legends

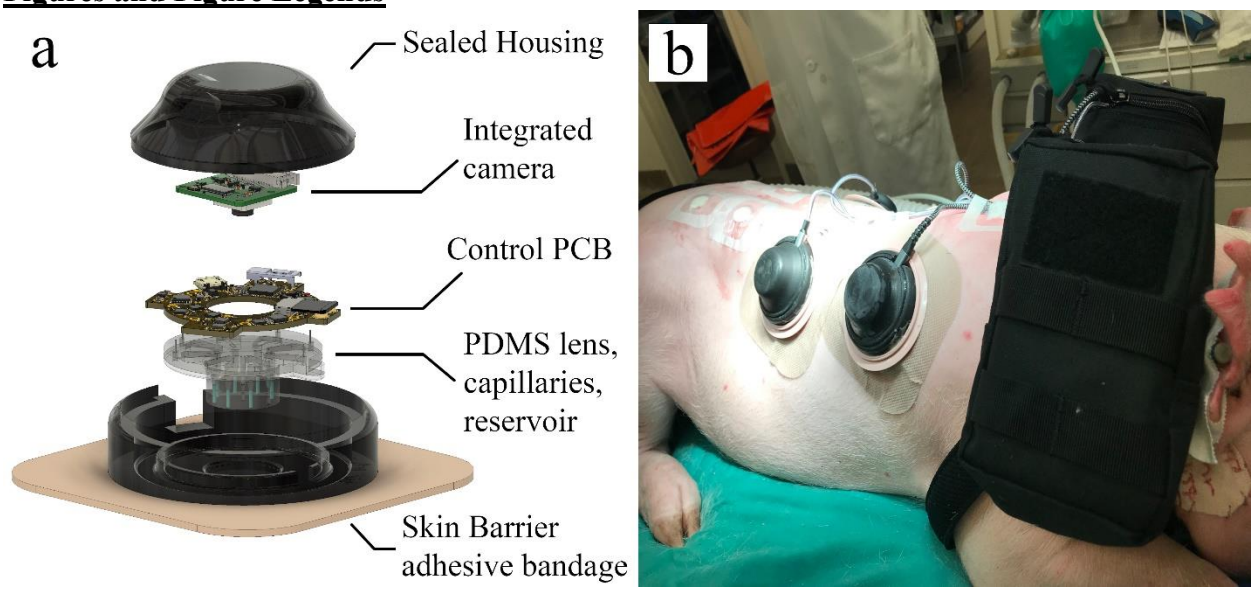

Figure 1 (a) An exploded diagram of the experimental device. (b) The experimental device applied to pig dorsal wounds in an experimental setting. Batteries are stored in pouches attached to the shoulder harness.

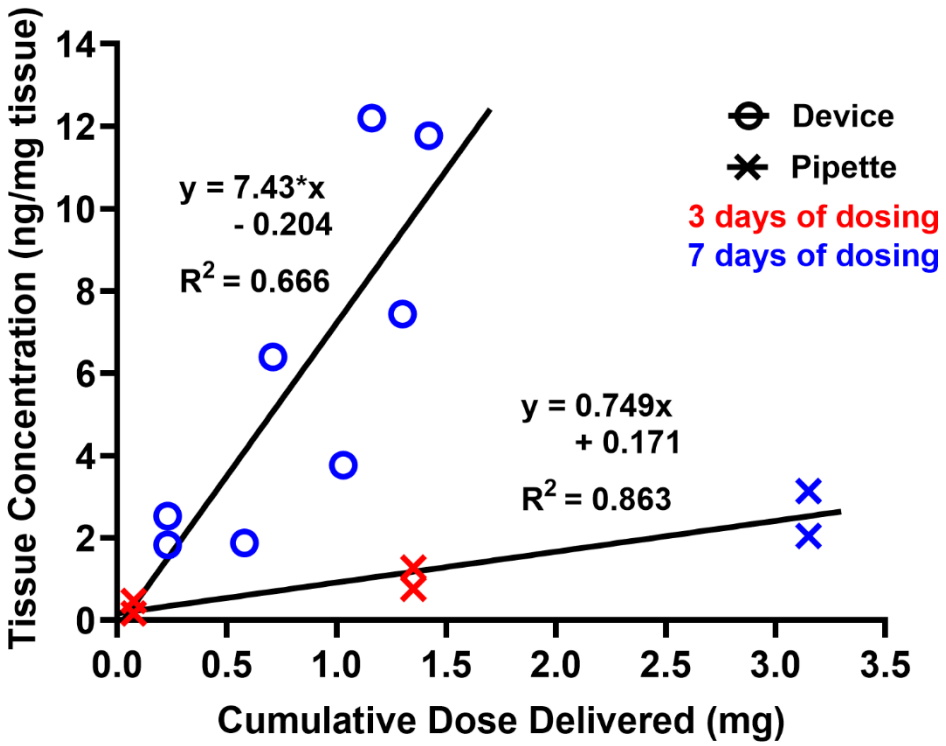

Figure 2 Tissue levels of fluoxetine in the wound following daily application using the experimental device or a pipette. Each data point represents one wound. Device, n=8 wounds; pipette, n=6 wounds.

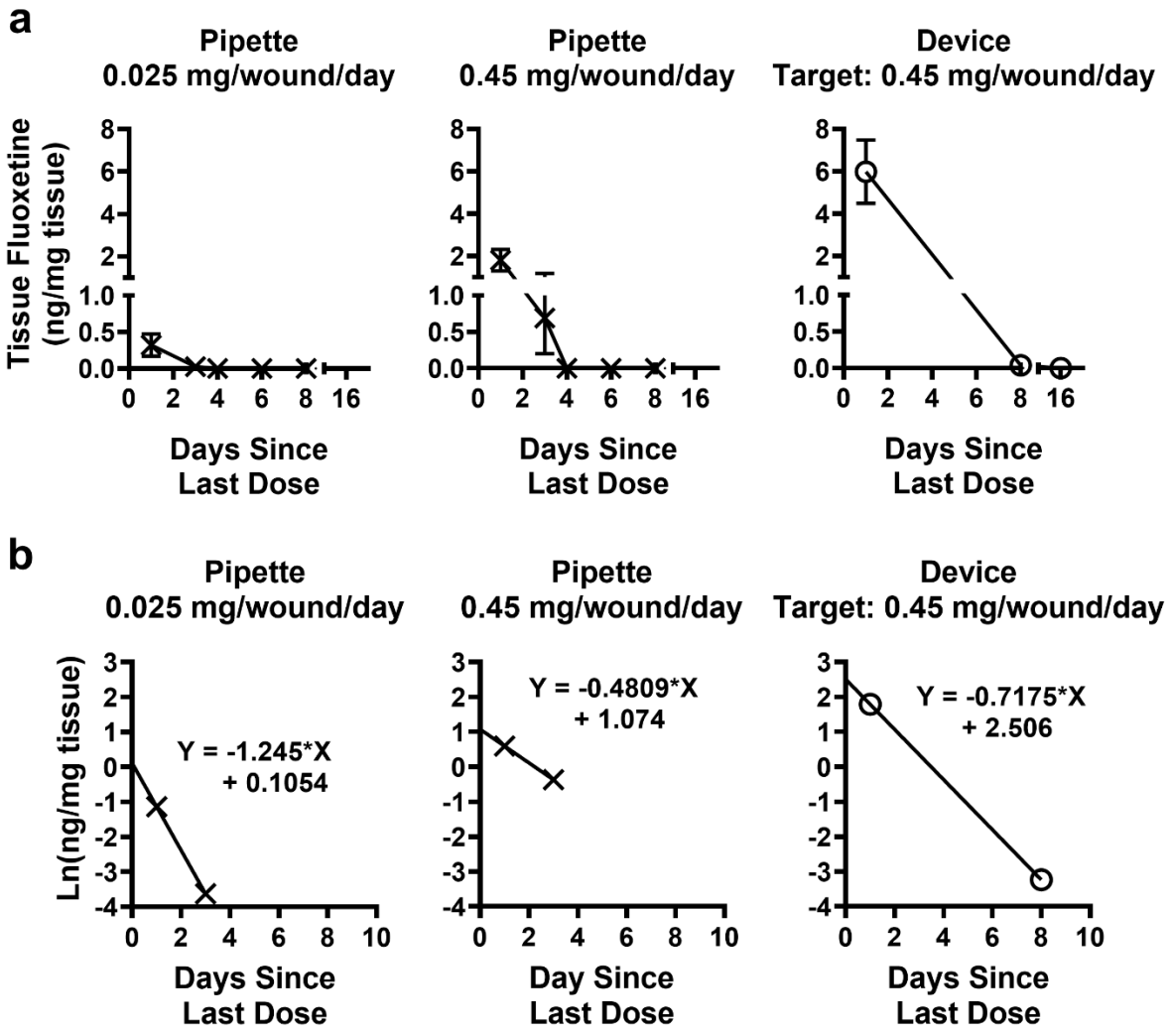

Figure 3 (a) Fluoxetine concentration in wound tissues collected on differing days post-treatment. Plots show mean ± standard error, n=2 to 8 wounds per point. (b) Plots of the natural logarithm of the tissue concentration across time for determination of the pharmacokinetic parameters.

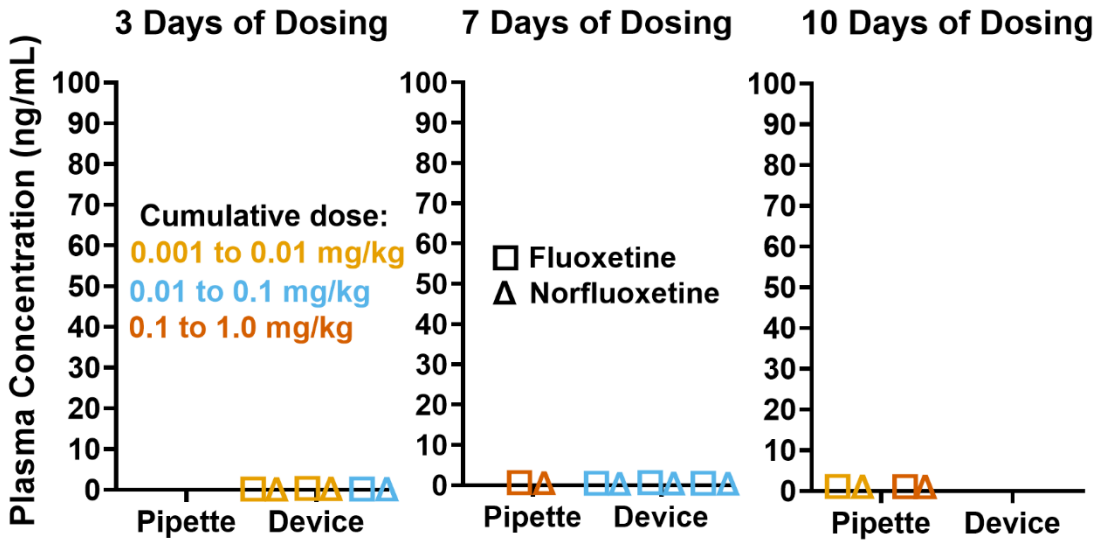

Figure 4 Fluoxetine and norfluoxetine concentrations in pig plasma (n=9 pigs) following topical fluoxetine wound treatment using the experimental device or a pipette. All results were below the limit of detection for the assay.

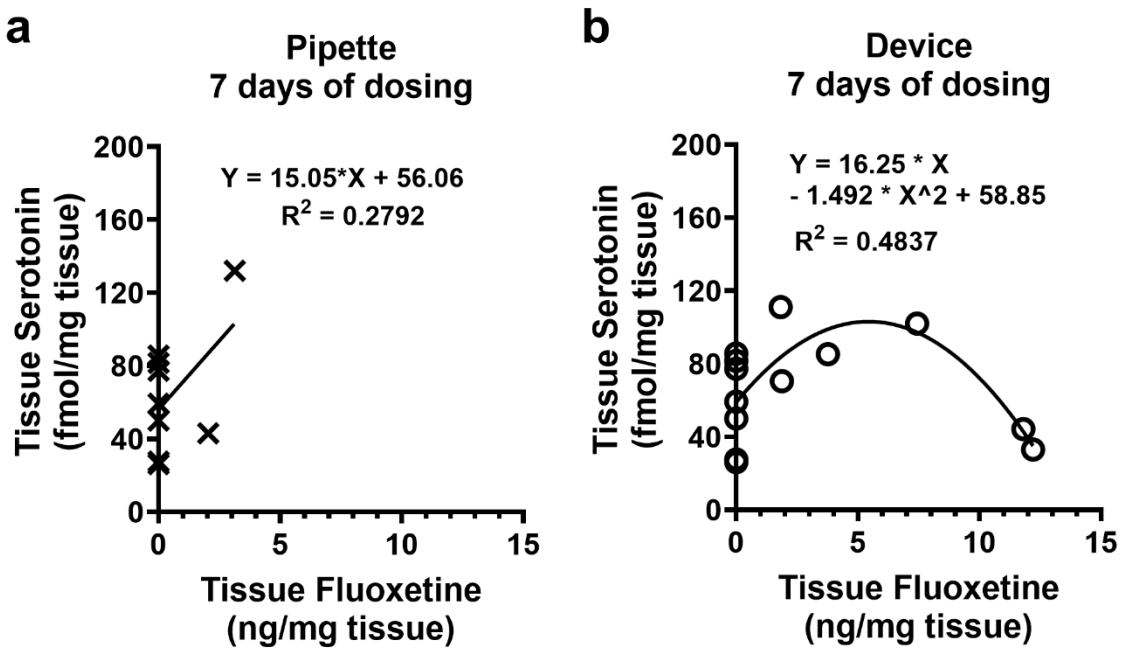

Figure 5 Wound tissue serotonin concentration after pipette (a) and device (b) topical fluoxetine wound treatment, plotted against the tissue fluoxetine level. Each data point represents one wound. Pipette, n=9 wounds; device, n=13 wounds.

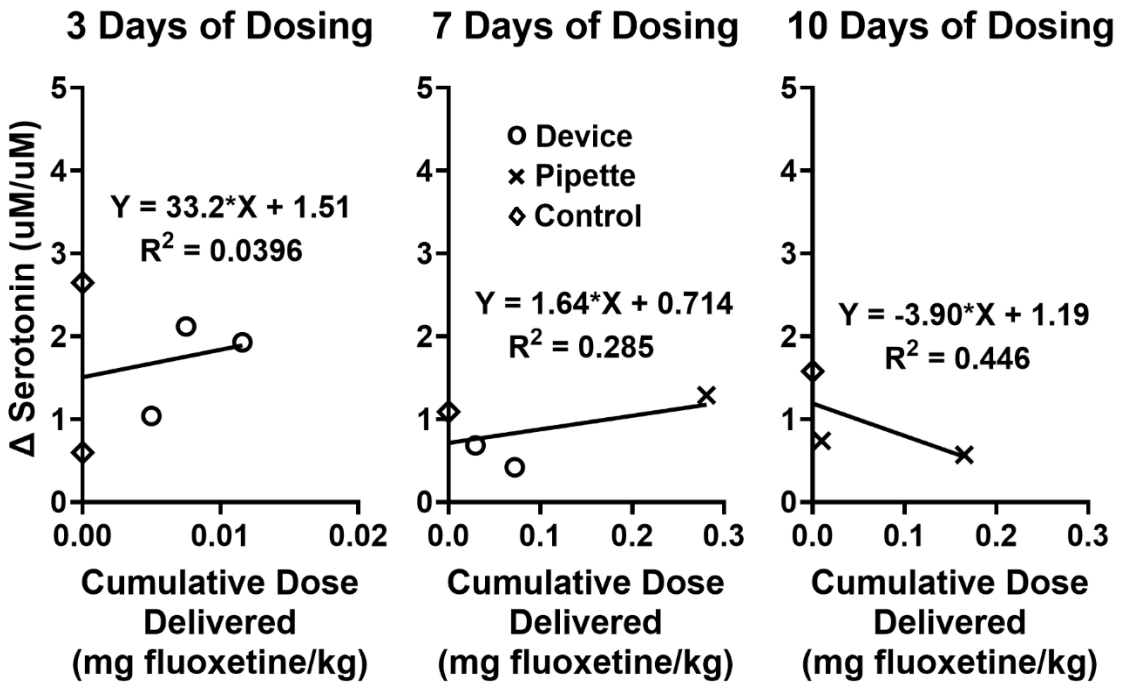

Figure 6 Changes in the plasma serotonin concentration after topical fluoxetine wound treatment using the experimental device or a pipette, plotted against the cumulative fluoxetine dose. Dose was normalized to the body weight of each pig. Each data point represents one pig. 3 days of dosing, n=5; 7 days, n=4; 10 days, n=3.

Tables

	Elimination constant (1/days)	Half-life (days)	Concentration at T_0 (ng/mg tissue)
Low dose pipette	1.245	0.5567	1.111
High dose pipette	0.4809	1.4413	2.926
Fluoxetine device	0.7175	0.9661	12.25

Table 1 Pharmacokinetic parameters of fluoxetine in the wound tissues.